HHS Public Access

Author manuscript

Cell. Author manuscript; available in PMC 2015 October 09.

Published in final edited form as:

Cell. 2014 October 9; 159(2): 306–317. doi:10.1016/j.cell.2014.09.010.

O-GlcNAc transferase enables AgRP neurons to suppress browning of white fat

Hai-Bin Ruan[1,2], **Marcelo O. Dietrich**[1,2,5,6], **Zhong-Wu Liu**[1,2], **Marcelo R. Zimmer**[1,2,6], **Min-Dian Li**[1,2,3], **Jay Prakash Singh**[1,2], **Kaisi Zhang**[1,2,3], **Ruonan Yin**[1,2], **Jing Wu**[1,2], **Tamas L. Horvath**[1,2,4,5,*], and **Xiaoyong Yang**[1,2,3,*]

[1]Program in Integrative Cell Signaling and Neurobiology of Metabolism, Yale University School of Medicine, 333 Cedar Street, New Haven, CT 06520, USA

[2]Section of Comparative Medicine, Yale University School of Medicine, 333 Cedar Street, New Haven, CT 06520, USA

[3]Department of Cellular and Molecular Physiology, Yale University School of Medicine, 333 Cedar Street, New Haven, CT 06520, USA

[4]Department of Obstetrics, Gynecology and Reproductive Sciences, Yale University School of Medicine, 333 Cedar Street, New Haven, CT 06520, USA

[5]Department of Neurobiology, Yale University School of Medicine, 333 Cedar Street, New Haven, CT 06520, USA

[6]Department of Biochemistry, Universidade Federal do Rio Grande do Sul, Porto Alegre, RS 93042, Brazil

SUMMARY

Induction of beige cells causes the browning of white fat and improves energy metabolism. However, the central mechanism that controls adipose tissue browning and its physiological relevance are largely unknown. Here we demonstrate that fasting and chemical-genetic activation of orexigenic AgRP neurons in the hypothalamus suppress the browning of white fat. O-linked β-N-acetylglucosamine (O-GlcNAc) modification of cytoplasmic and nuclear proteins regulates fundamental cellular processes. The levels of O-GlcNAc transferase (OGT) and O-GlcNAc modification are enriched in AgRP neurons and are elevated by fasting. Genetic ablation of OGT in AgRP neurons inhibits neuronal excitability through the voltage-dependent potassium channel, promotes white adipose tissue browning, and protects mice against diet-induced obesity and

*To whom correspondence should be addressed: Section of Comparative Medicine, Yale University School of Medicine, P.O. Box 208016, New Haven, CT 06520-8016. Tel: 1-203-737-1446; Fax: 1-203-785-7499; xiaoyong.yang@yale.edu or tamas.horvath@yale.edu.

AUTHOR CONTRIBUTIONS

H.-B.R. designed and performed most of the experiments. Z.-W.L. designed and performed electrophysiological studies. M.O.D. and T.L.H. generated essential animal models and designed and executed experiments. M.R.Z. performed ribosome-mRNA profiling. M.L., J.P.S., K.Z., R.Y. and J.W. assisted in experiments. X.Y. conceived, designed and supervised the project. H.-B.R. and X.Y. wrote the manuscript.

insulin resistance. These data reveal adipose tissue browning as a highly dynamic physiological process under central control, in which O-GlcNAc signaling in AgRP neurons is essential for suppressing thermogenesis to conserve energy in response to fasting.

INTRODUCTION

Overweight and obesity develop when energy intake exceeds energy expenditure, storing excess calories in the adipose tissue (Spiegelman and Flier, 2001). The adipose organ comprises white (WAT) and brown adipose tissues (BAT). WAT primarily stores energy as triglycerides and its excess and dysfunction lie at the core of obesity and associated metabolic disorders. In contrast, BAT-mediated adaptive thermogenesis dissipates chemical energy as heat, and protects against obesity in both rodents and humans (Cinti, 2012; Kajimura and Saito, 2013; Nedergaard et al., 2010; Smorlesi et al., 2012). Emerging evidence has demonstrated that “brown-like” adipocytes, so-called beige/brite cells, exist in specific WAT depots and differ from classic brown adipocytes in their origin and molecular identity (Petrovic et al., 2010; Rosen and Spiegelman, 2014; Wu et al., 2012). Multiple intrinsic factors and secreted molecules have been identified that modulate the development and function of beige/brite adipocytes and thus metabolic health in animals (Bartelt and Heeren, 2013; Wu et al., 2013). However, whether and how the central nervous system controls WAT browning is almost completely unknown.

In the arcuate nucleus of the hypothalamus resides orexigenic neurons expressing agouti-related protein (AgRP)/neuropeptide Y (NPY) and anorexigenic neurons expressing proopiomelanocortin (POMC). These neurons are regulated by peripheral hormones and nutrients, and are critical for maintenance of energy homeostasis and glucose metabolism. During food deprivation, AgRP neurons are strongly activated to promote hunger (Hahn et al., 1998; Liu et al., 2012; Takahashi and Cone, 2005), an effect vastly mediated by ghrelin signaling in these neurons (Andrews et al., 2008; Chen et al., 2004; Yang et al., 2011). Despite the involvement of other hypothalamic areas in the control of thermogenesis in classic BAT (Nogueiras et al., 2008; Scherer and Buettner, 2011; Yasuda et al., 2004), it is not known whether hunger-promoting AgRP neurons are involved in the control adaptive thermogenesis and/or browning of WAT.

Thousands of cytoplasmic and nuclear proteins are modified by a single O-linked β-N-acetylglucosamine (O-GlcNAc) moiety at serine or threonine residues, termed O-GlcNAcylation (Hart et al., 2007; Torres and Hart, 1984). This dynamic and reversible modification is emerging as a key regulator of diverse cellular processes, such as signal transduction, transcription, translation, and proteasomal degradation (Love and Hanover, 2005; Ruan et al., 2013a; Yang et al., 2002). Perturbations in protein O-GlcNAcylation are implicated in various human diseases including diabetes mellitus, neurodegeneration and cancer (Hart et al., 2007; Love and Hanover, 2005; Ruan et al., 2013b). Key components of insulin signaling can be O-GlcNAcylated (Ruan et al., 2013b; Whelan et al., 2010), and O-GlcNAcylation is a negative regulator of insulin signaling (Yang et al., 2008). Transgenic mice overexpressing OGT in skeletal muscle and fat exhibit elevated circulating insulin levels and insulin resistance (McClain et al., 2002). O-GlcNAcylation of transcription

factors and cofactors such as FOXO1, CRTC2 and PGC-1α promotes the expression of gluconeogenic genes in liver (Dentin et al., 2008; Housley et al., 2008; Housley et al., 2009; Ruan et al., 2012). These studies demonstrate a vital role for O-GlcNAc signaling in metabolic regulation in peripheral tissues. However, the central roles of O-GlcNAc signaling in metabolic regulation have not been explored.

Here, we show that OGT expression is enriched in hypothalamic AgRP neurons and induced by fasting and ghrelin. Pharmacogenetical activation of AgRP neurons suppresses the thermogenic program in WAT, while the selective knockout of *Ogt* in AgRP neurons inhibits neuronal activity, promotes WAT browning, and protects mice against diet-induced obesity.

RESULTS

Fasting suppresses thermogenic program in WAT

A major component of energy homeostasis is to adjust energy expenditure according to the level of energy intake (Apfelbaum et al., 1971; Shibata and Bukowiecki, 1987; Welle and Campbell, 1983). Given that WAT browning is an emerging regulator of energy expenditure, we test whether food availability regulates the browning process. Four adipose depots including classic BAT, gonadal WAT (gWAT), and two major depots that have the potential of browning -retroperitoneal and inguinal WAT (rWAT and iWAT) - from *ad libitum* fed and 24 h-fasted mice were collected (Fisher et al., 2012; Guerra et al., 1998; Nedergaard and Cannon, 2013). Fasting reduced total RNA level in most depots (Figure S1A), thus thermogenic gene expression was determined by relative real-time PCR and calculated as total level per depot (Nedergaard and Cannon, 2013). *Ucp1* expression was significant decreased in BAT and rWAT (Figure 1A and B), and showed a tendency of reduction in iWAT and gWAT in fasted mice as compared to fed controls (Figure 1C and S1B). The expression of other thermogenic genes including *Ppargc1a*, *Prdm16*, *Cidea*, and *Dio2* during fasting was significantly suppressed in rWAT, but mainly unchanged in BAT, iWAT, and gWAT (Figure 1A–C and Figure S1B). These data suggest that rWAT is the major depot responsible for the inhibitory effect of fasting on thermogenesis.

Cold exposure has been extensively shown as a physiological stimulator of BAT activation and WAT browning (Cinti, 2012). However, cold exposure did not efficiently induce *Ucp1* transcription in any fat depots when animals were deprived of food, indicating that fasting diminishes the effect of cold on thermogenesis (Figure 1D and S1C). When we examined the levels of Ucp1 protein in these fat depots, we found that fasting downregulated Ucp1 in rWAT but not in BAT and iWAT (Figure 1E). Sympathetic outflow to BAT and WAT controls the expression of thermogenic genes and heat production in brown and beige fat (Harms and Seale, 2013). Thus we hypothesized that changes in sympathetic nerve activity in respond to stimuli determine the thermogenic program in different depots. Fasting increased levels of norepinephrine (NE) in serum (Figure S1D), BAT and iWAT (Figure 1F, G). However, NE level only in rWAT was decreased during fasting (Figure 1H), correlated with the reduction in thermogenic gene expression. Fasting also dampened the induction of NE level in rWAT by cold (Figure 1H). In addition, fasting downregulated while cold upregulated the levels of tyrosine hydroxylase (TH), a marker of sympathetic nerve, and

ubiquitin carboxyl-terminal esterase L1 (Uchl1), a general marker for peripheral neurons in rWAT (Figure 1E) (Burgi et al., 2011; Wilkinson et al., 1989). Taken together, these data suggest that fasting controls sympathetic outflow and regulates browning in rWAT.

Acute activation of AgRP neurons suppresses thermogenic program in WAT

Orexigenic AgRP/NPY neurons in the hypothalamus are critical for energy homeostasis and glucose metabolism in response to nutrient and hormonal cues (Belgardt et al., 2009). During fasting, the activation of AgRP neurons provokes animals to seek food and simultaneously suppresses energy expenditure (Dietrich and Horvath, 2012; Small et al., 2001). To determine whether AgRP neurons regulate WAT browning, we took advantage of a chemical genetics approach that allows acute, cell type-specific control of neuronal activity in vivo. Specifically, we generated mice only expressing the cation channel Trpv1 in AgRP neurons (Figure 2A) (Arenkiel et al., 2008). Capsaicin is a Trpv1 agonist that will induce the depolarization and activation of AgRP neurons in *Trpv1*$^{-/-}$*;AgRP-Cre*$^{+}$*;R26*^{Trpv1} mice. Acute activation of AgRP neurons by systemic injection of capsaicin (10 mg/kg, i.p.) for only 1 h strongly inhibited the expression of thermogenic genes including *Ucp1*, *Ppargc1a*, *Prdm16* and *Cidea* in rWAT, and to a less extent in iWAT, but not in classic BAT or visceral gWAT in *Trpv1*$^{-/-}$*;AgRP-Cre*$^{+}$*;R26*^{Trpv1} mice (Figure 2B). Activation of AgRP neurons significantly reduced energy expenditure in *Trpv1*$^{-/-}$*;AgRP-Cre*$^{+}$*;R26*^{Trpv1} mice, compared to *Trpv1*$^{-/-}$*;AgRP-Cre*$^{-}$*;R26*^{Trpv1} mice (Figure 2C). Food was removed during these studies to eliminate the effect of diet-induced thermogenesis. Thus far, these data indicate that acute activation of AgRP neurons decreases energy expenditure and thermogenenic gene expression profile in selected fat depots.

To test the physiological importance of AgRP neuron-regulated browning, capsaicin-injected mice were immediately placed at 4 °C. Core body temperature dropped lower in *Trpv1*$^{-/-}$*;AgRP-Cre*$^{+}$*;R26*^{Trpv1} mice (Figure 2D), suggesting that AgRP activation inhibits cold-induced thermogenesis. Gene expression analyses showed that cold promoted *Ucp1* transcription in BAT (Figure 2E), but not in rWAT (Figure 2F) of *Trpv1*$^{-/-}$*;AgRP-Cre*$^{+}$*;R26*^{Trpv1} mice, indicating that thermogenic program in rWAT is specifically inhibited by AgRP neurons. Acute activation of AgRP neurons did not change serum levels of NE (Figure 2G). However, we observed a reduction of NE level specifically in rWAT of *Trpv1*$^{-/-}$*;AgRP-Cre*$^{+}$*;R26*^{Trpv1} mice (Figure 2H). Treatment with a selective β3 agonist, CL-316, 243 rescued the decrease in body temperature and *Ucp1* expression in rWAT of capsaicin-injected *Trpv1*$^{-/-}$*;AgRP-Cre*$^{+}$*;R26*^{Trpv1} mice (Figure 2I and J). These data demonstrate that acute activation of hunger-promoting AgRP neurons suppresses browning in rWAT by regulating sympathetic activity.

OGT controls AgRP neuronal activity

We then sought to determine possible nutrient sensors in AgRP neurons that respond to fasting. Previously, we have shown that O-GlcNAcylation of insulin signaling proteins and transcriptional regulators in peripheral tissues is important for glucose and lipid metabolism (Li et al., 2013; Ruan et al., 2012; Ruan et al., 2013b; Yang et al., 2008). Expression of OGT and overall O-GlcNAc levels (Figure S2A, B) in the hypothalamus are significantly higher than peripheral tissues such as liver, WAT and muscle. However, little is known about the

role of O-GlcNAc modification in the hypothalamic regulation of metabolism. To determine the relative levels of *Ogt* transcripts in AgRP neurons, we isolated AgRP neuron-specific ribosome-associated mRNAs from the arcuate nucleus of *AgRP-Cre*$^{+}$*;RPL22*^{HA} mice by immunoprecipitation of the actively translating polyribosomes that were tagged with hemagglutinin (HA) epitope (Sanz et al., 2009). *Ogt* transcripts showed a 4-fold enrichment in AgRP neurons (Figure 3A). Consistently, immunohistochemistry demonstrated that a subset of AgRP/NPY neurons have relatively high levels of OGT proteins and O-GlcNAcylation (Figure 3B and C). Food deprivation for 24 h increased OGT expression and O-GlcNAc levels in AgRP neurons (Figure 3B and C). Ghrelin is a hormone released by the empty stomach that promotes hunger by activating AgRP neurons in the hypothalamus (Andrews et al., 2008; Chen et al., 2004; Liu et al., 2012; Luquet et al., 2007; Wiedmer et al., 2011). We found that ghrelin increased O-GlcNAc levels in AgRP neurons (Figure 3D) and reduced levels of Ucp1 protein in rWAT (Figure S2C). These data point to the possibility that O-GlcNAcylation functions as a fasting signal in AgRP neurons.

To determine the physiological role of O-GlcNAc signaling in AgRP neurons, we generated AgRP neuron-specific *Ogt* knockout (KO) mice (Figure S2D). Immunofluorescent staining of OGT on *Npy-hrGFP* hypothalamus showed that OGT was specifically deleted in AgRP neurons (Figure S2E). Real-time PCR and western blot analyses confirmed that OGT was not ectopically deleted in the whole hypothalamus, cortex, or other peripheral metabolic tissues (Figure S2F and G). To identify AgRP neurons during electrophysiological studies, *AgRP-Ogt* KO mice were cross-bred into the *Npy-hrGFP* background (Figure 3E). Whole-cell current clamp measurements demonstrated that the membrane potential of AgRP neurons was similar between control (CT) and KO mice (Figure 3F). However, the spontaneous firing rate was reduced in KO mice (Figure 3G and H).

OGT modulates the potassium channel in AgRP neurons

Voltage-dependent potassium (K_V) channels mediate the repolarization and after-hyperpolarization phases of action potential, and defects in K_V current lead to dampened activity but intact membrane potential in neurons (Bean, 2007). Electrophysiological analyses showed a reduction in outward K^+ current in AgRP neurons from KO mice compared to CT mice (Figure 4A, B). The K^+ current in AgRP neurons was slowly inactivated, suggesting a possible involvement of delayed rectifier K_V channels. Kcnq3 (K_V7.3), mediating delayed rectifier K^+ current, is expressed in AgRP neurons (Ren et al., 2012). We found that OGT interacted with Kcnq3 in the hypothalamus, and fasting enhanced their interaction (Figure 4C). Kcnq3 has been shown to be O-GlcNAc-modified at murine synapse (Trinidad et al., 2012), and mutation of the O-GlcNAc site Threonine 655 to Alanine (T655A) almost abolished the O-GlcNAcylation on Kcnq3 (Figure 4D). Then we assessed Kcnq3 activity, and found that T655A mutant channel showed a significant reduction in K^+ current compared to the wildtype Kcnq3 (Figure 4E and F), suggesting that O-GlcNAcylation of this K_V channel is a key regulatory mechanism underlying cellular excitability. Taken together, *AgRP-Ogt* KO mice are intrinsically defective in the activity of K_V channels and neuronal firing, serving as a model to study metabolic roles of AgRP neurons.

Ogt knockout in AgRP neurons promotes a thermogenic program in WAT

Acute activation of AgRP neurons specifically suppressed rWAT browning (Figure 2), thus we hypothesized that impaired AgRP neuronal activity in *AgRP-Ogt* knockout mice would induce a thermogenic gene program in rWAT. As expected, levels of *Ucp1* and *Cidea* mRNA were significantly increased in rWAT (Figure 5A), but remained unchanged in BAT of KO mice, compared to CT mice (Figure 5B). Consistently, uncoupled oxygen consumption rate (OCR) in BAT stayed the same, while uncoupled OCR in rWAT was higher, when comparing KO mice to CT mice (Figure 5C). Blocking the β3 adrenergic receptor by SR59230A restored the *Ucp1* expression in rWAT (Figure 5D), strengthening the notion that AgRP neurons control rWAT browning through SNS.

BAT of KO mice remained susceptible to the suppression of thermogenic genes by fasting (Figure 5E, compared to Figure 1A). In contrast, this suppression was abolished in rWAT of KO mice (Figure 5F, compared to Figure 1B). Ghrelin also failed to downregulate Ucp1 protein levels in rWAT of KO mice (Figure S3A). These data demonstrate that O-GlcNAc signaling in AgRP neurons is required for the regulation of WAT browning by fasting and ghrelin. As a result, *AgRP-Ogt* KO mice showed less reduction in energy expenditure than CT mice during the first 24 h of fasting (Figure 5G) with concomitant increase in weight loss (Figure 5H). Nevertheless, there was no significant reduction in body weight of *ad libitum* KO mice (Figure S3B).

The defect in AgRP neuronal activity is normally associated with decreased feeding behavior (Dietrich et al., 2010). However, there was no change in food intake in *AgRP-Ogt* KO mice (Figure S3C). This is possibly due to the overproduction of *Agrp* and *Npy* transcripts via unknown compensatory mechanisms (Figure S3D), and/or that the OGT-positive subset of AgRP neurons does not directly modulate feeding. Cold exposure did not affect OGT expression in AgRP neurons (Figure S3E), and *AgRP-Ogt* KO mice and control mice under fed conditions showed similar core body temperature during cold challenge (Figure S3F), indicating that the silencing of AgRP neurons either by feeding or by OGT deletion abolishes the impact of this neural circuit on cold-induced thermogenesis.

It is reported that AgRP neurons regulate hepatic gluconeogenesis and that the browning of WAT improves glucose metabolism in mice (Könner et al., 2007; Qian et al., 2013; Seale et al., 2011). We observed a decrease in hepatic expression of gluconeogenic genes including *Ppargc1a*, *G6pc*, and *Pck1* in KO mice (Figure 5I). Gluconeogenesis in AgRP-OGT KO mice was downregulated as shown by decreased blood glucose levels during pyruvate tolerance test and glucose tolerance test (Figure 5J and K). No changes in insulin levels or insulin sensitivity were observed (Figure S3G and H). These data demonstrate that *Ogt* knockout in AgRP neurons improves glucose metabolism in mice.

Ogt knockout in AgRP neurons protects against diet-induced obesity and insulin resistance

Next, we challenged the mice with high fat diet (HFD). Consistent with the findings in mice on NC, thermogenic genes including *Ucp1*, *Ppargc1a*, *Prdm16* and *Cidea* were dramatically increased in rWAT of AgRP-OGT KO mice (Figure 6A). There were more “brown-like”

adipocytes and less fat exist in rWAT of KO mice (Figure 6B and C). Although BAT and iWAT showed a reduction in fat weight and content (Figure 6B and C), the expression of thermogenic genes was comparable between KO and CT groups (Figure 6A). We did not observe any changes in weight, morphology or gene expression in gWAT (Figure 6A–C). We also observed that protein levels of Ucp1 and tyrosine hydroxylase were markedly elevated in rWAT of KO mice (Figure 6D). These mice also exhibited increased NE levels in rWAT but not in BAT or iWAT (Figure 6E). These data demonstrate that *Ogt* knockout in AgRP neurons selectively activates browning in rWAT of mice fed on HFD.

Consistent with the activated thermogenic program, heat production in KO mice was significantly increased compared to CT mice, as demonstrated by the metabolic cage study (Figure 6F). As a result, both female and male KO mice gained significantly less body weight and fat mass compared to CT mice (Figure 7A, B and Figure S4A, B), despite consuming a similar amount of HFD (Figure 7C). Although levels of fasting glucose and insulin were not significantly different (Figure 7D, E and Figure S4C, D), there was a reduction in the values of the homeostasis model assessment of insulin resistance (HOMA-IR) in both female and male KO mice (Figure 7F and Figure S4E). Consistent with these observations, glucose tolerance test and insulin tolerance test showed that *AgRP-Ogt* KO mice were more glucose tolerant and insulin sensitive than CT mice (Figure 7G, H, and Figure S4F). Taken together, these data reveal that *Ogt* deficiency in AgRP neurons increases WAT browning and protects mice from diet-induced obesity and insulin resistance.

DISCUSSION

Studies in the past few years have greatly expanded our knowledge of beige adipocytes. There is no doubt that beige fat is metabolically important, especially during cold exposure and nutrient overload. Stimulating the browning process protects mice from diet-induced obesity, whereas the ablation of beige adipoctyes causes metabolic dysfunction (Cohen et al., 2014; Seale et al., 2011). In this study, we identify fasting as a negative, physiological regulator of the thermogenic program in beige adipocytes. Intriguingly, fasting diminishes the effect of cold exposure on thermogenesis, suggesting that fasting is a predominant regulator of browning in order to conserve energy for survival.

Hypothalamus has been long proposed to regulate adaptive thermogenesis in BAT, independently on its regulation on food intake (Kong et al., 2012; Vogt and Bruning, 2013). Neuropeptides AgRP and NPY have been shown to inhibit BAT function, while α-MSH increases SNS activity and BAT function (Shi et al., 2013; Yasuda et al., 2004). It is not known whether these circuits also control WAT browning. In this study, we demonstrate that chemical-genetic activation of AgRP neurons acutely suppresses the thermogenic program in beige fat, demonstrating that white fat browning is a highly dynamic and reversible process. Conversely, impairment in AgRP neuronal activity abolishes fasting-mediated inhibition of WAT browning. These results reveal the dynamic nature of WAT browning and identify a specific neuronal population that negatively regulates this process.

Fasting and AgRP neuronal activation appear to regulate browning preferentially in rWAT, to a much less extent in other WAT depots but not in BAT. We demonstrate that uniquely in rWAT, sympathetic nerve activity correlates with thermogenic gene expression and browning during cold and fasting stimuli. In this regard, mapping the neuronal circuits linking AgRP neurons to sympathetic innervation onto different WAT depots would provide further insights. It is also possible that other mechanisms may mediate the effect of AgRP neurons on WAT browning. Although as a relative small depot, rWAT responds much quicker than BAT and other WAT depots after cold exposure or food deprivation. This suggests that browning in rWAT may function as a first line of defense to maintain energy homeostasis when food and environmental temperature are fluctuant.

O-GlcNAc signaling has long been proposed as a nutrient sensor in multiple peripheral tissues. Hyperglycemia-associated elevation in O-GlcNAc levels mediates many aspects of glucotoxicity (Ruan et al., 2013b). On the other hand, O-GlcNAc levels can also be increased by glucose deprivation in several cell types (Cheung and Hart, 2008; Kang et al., 2009; Taylor et al., 2008). Consistent with the latter observations, we demonstrate that OGT expression and O-GlcNAc modification increase in AgRP neurons in response to fasting and ghrelin, although the molecular mechanism has yet to be defined. Genetic ablation of OGT in AgRP neurons promotes WAT browning, thus leading to improved glucose and energy metabolism. Mouse models with defective BAT often fail to maintain their body temperature upon cold exposure (Feldmann et al., 2009). However, OGT expression in AgRP is not affected by cold, and *AgRP-Ogt* KO mice maintain a normal core temperature upon cold exposure. These observations prompt the hypothesis that brown fat primarily maintains homeothermy to combat cold, whereas beige fat regulates energy metabolism in response to nutrient stress. This notion is supported by the recent finding that PRDM16 ablation in beige fat does not affect body temperature in mice (Cohen et al., 2014).

Neuronal circuits in the arcuate nucleus of the hypothalamus are relatively tolerant to perturbations, especially during developmental and neonatal stages. Neonatal ablation of AgRP neurons has minimal effects on feeding, although ablation of these neurons in adults causes rapid starvation (Luquet et al., 2005). Genetic knockout of *Agrp* gene in mice also does not affect food intake (Qian et al., 2002). These data suggest that neuronal plasticity can compensate for the loss of *Agrp* gene or AgRP neurons. In our study, the deletion of *Ogt* in AgRP neurons occurs early during development. Although neuronal activity is decreased in *AgRP-Ogt* KO mice, the expression of *Agrp* and *Npy* transcripts is elevated, which may contribute to the maintenance of normal food intake.

Hunger and cold are two life-history variables during the development and evolution of mammals. We have observed that food deprivation (the negative regulator) dominates over cold exposure (the positive regulator) in the central control of WAT browning. This regulatory system may be evolutionarily important as it can reduce heat production to maintain energy balance during fasting. Modulating the hypothalamic control of WAT browning represents a potential strategy to combat obesity and associated morbidity.

EXPERIMENTAL PROCEDURES

Mice

Ogt-floxed mice on C57BL/6 background (Shafi et al., 2000) were kindly provided by Dr. Steven Jones (University of Louisville). *AgRP-Cre* mice, kindly donated by Alison Xu (University of California San Francisco), have been maintained in our colony on a mixed background (Xu et al., 2005). *Trpv1*^{tm1Jul}/J mice (#003770), *Gt(ROSA)26Sor*$^{tm1(Trpv1,ECFP)Mde}$/J (#008513) and *Npy-hrGFP* mice (#006417), which express humanized *Renilla* GFP under the control of the mouse *Npy* promoter, were from Jackson Laboratory. To express Trpv1 selectively in AgRP neurons, we have bred both Trpv1 colonies to a second *AgRP-Cre* line (*Agrp*$^{tm1(cre)Lowl}$/J, #012899, Jackson Laboratory). All animals were kept on a 12 h: 12 h light: dark cycle. Mice were free to access water and either fed on a standard chow diet or 60% high fat diet (Research Diets). 10 mg/kg body weight (BW) of capsaicin, 1 mg/kg BW of CL-316, 243 (R&D Systems), and 120 mmol/kg BW of ghrelin (Enzo) were i.p. injected when indicated. Indicated mice were treated with 5 mg/kg BW of SR59230A (Abcam) for 3 consecutive days, and tissues were collected 2h after the final injection.

Metabolic assays

Body weights were recorded every week. Body composition was assessed using an EchoMRI system. For food intake measurement, mice were individually housed for at least 1 week for environmental habituation, and food consumption was weighed every morning for 7 consecutive days. For the metabolic cage study, mice were acclimated in metabolic chambers (TSE Systems) for 3 days, and then gas exchange, food intake, and ambulatory activity were recorded continuously for another 3 days. Heat production was calculated and adjusted to body weight (Tschop et al., 2012). Body temperature was measured rectally using a thermo-coupler (Physitemp). For pyruvate-, glucose-, and insulin- tolerance tests. 16 h fasted mice were injected with intraperitoneally with sodium pyruvate (1.5 g/kg body weight) or glucose (1.5 g/kg body weight); 6 h fasted mice were injected with insulin (1 U/kg body weight). Blood glucose from tail-vein blood collected at the designated times was measured using a Nova Max Glucometer. Insulin (Millipore) and norepinephrine (Abnova) were determined using ELISA kits.

Electrophysiology

Mice were anaesthetized with isofluorane and sacrificed by decapitation. The brain was gently removed from the skull, and chilled in 4°C oxygenated high-sucrose solution containing (mM): sucrose 220, KCl 2.5, NaH_2PO_4 1.23, $NaHCO_3$ 26, $CaCl_2$1, $MgCl_2$ 6 and glucose 10, pH 7.3 with NaOH. The brain was trimmed to a large block containing the hypothalamus and then sliced on a vibrating microtome. Coronal, 300 μm, slices are cut through the full extent of the arcuate nucleus/lateral hypothalamus. Slices are maintained in artificial cerebrospinal fluid (ACSF, containing in mM: NaCl, 126; KCl, 2.5; MgCl2, 1.2; CaCl2.2H2O, 2.; NaH2PO4.H2O, 1.2; NaHCO3, 26; Glucose, 10) for 1 hr at room temperature in 95% O2 5% CO2 saturated ACSF prior to recordings. Perforated whole-cell current clamp were used to observe spontaneous action potentials. Slices were maintained at 34°C and perfused continuously with ASCF (bubbled with 5% CO2 and 95% O2)

containing (in mM): NaCl, 124; KCl, 3; CaCl2, 2; MgCl2, 2; NaH2PO4, 1.23; NaHCO3, 26; Glucose, 2.5; pH 7.4 with NaOH.. All data were sampled at 3–10 kHz and filtered at 1–3 kHz. Whole-cell voltage clamp were used to record KV currents with a Multiclamp 700B amplifier. The patch pipette was made of borosilicate glass with a Sutter puller. The tip resistance of the recording pipettes was 2–4 MΩ after filling with a pipette solution containing (mM): The pipette solution contained (mM): potassium methanesulfonate 135, $MgCl_2$ 2, HEPES 10, EGTA 1.1, Mg-ATP 2, and Na_2-phosphocreatin 10, Na_2-GTP 0.3, pH 7.3 with KOH. Cells were held at −80 mV and step depolarized to +40 mV with 10 mV increments. All data were sampled and analyzed with Axograph X.

Ribosome RNA enrichment

For ribosome profiling, the methods used here were in accordance with the original description of the animal model with minor modifications (Dietrich et al., 2013; Sanz et al., 2009). Fifty days old mice (from both genders) were sacrificed and 5–6 hypothalami were pooled for each N. A total of N = 4 was used. After RNA isolation, we obtained approximately 25 ng of RNA per sample. Only samples with high enrichment for *Agrp* and *Npy* were used for *Ogt* gene expression analyzes.

RNA and real time PCR

Total RNA was extracted from mouse tissues using TRIzol reagent (Invitrogen). cDNA was reverse transcribed (Bio-Rad) and amplified with SYBR Green Supermix (Bio-Rad) using a LightCycler 480 Real-time PCR system (Roche). All data were normalized to the expression of *18s* and *36b4*. Primer sequences are available on request. When comparing gene expression between fed and fasted animals, total amounts of mRNA were calculated based on relative mRNA levels and total amounts of RNA isolated from specific depots (Nedergaard and Cannon, 2013).

Cell Culture

HEK 293T cells were cultured in DMEM with 10% fetal bovine serum (FBS). Transfection was performed using FuGENE HD (Promega) according to the manufacture's manual. For immunoprecipitation, whole-cell lysates were mixed with the Myc antibody and precipitated by Protein A/G agarose beads (Santa Cruz).

Western blotting

Anti-OGT (ab96718), anti-O-GlcNAc (RL2, ab2739), and anti-UCP1 (ab10983) were from Abcam. Anti-Tyrosine hydroxylase (#2792) and anti-UCHL1 (#3524) were from Cell Signaling Technology. Anti-Myc (sc-40) was from Santa Cruz Biotechnology. Tissues were lysed in buffer containing 1% Nonidet P-40, 50 mM Tris·HCl, 0.1 mM EDTA, 150 mM NaCl, proteinase inhibitors and protein phosphatase inhibitors. Equal amounts of protein lysate were electrophoresed on SDS-PAGE gels and transferred to PVDF membrane. Primary antibodies were incubated at 4 °C for overnight. Western blotting was visualized by peroxidase conjugated secondary antibodies and ECL chemiluminescent substrate.

Histology

Mice were anesthetized for intracardial perfusion of PBS, followed by 4% paraformaldehyde. Brain and adipose depots were dissected and post-fixed in 4% paraformaldehyde overnight. Coronal brain sections (50 μm) were prepared using a vibrating microtome. Paraffin sections of fat tissues were stained with Haematoxylin & Eosin (H&E). For immunofluorescence, tissue slides were blocked with 3% BSA, 0.2% TWEEN 20 in PBS, incubated with primary antibodies (1:100 dilution) overnight, and secondary antibodies (Alexa Fluor 488 anti-Rabbit IgG, Alexa Fluor 594 anti-Rabbit IgG, and Alexa Fluor 594 anti-Mouse IgG, 1:400) for 1h. An Olympus confocal system was used for fluorescence detection.

Statistical analyses

Results are shown as mean ± SEM. The comparisons were carried out using two-tailed unpaired Student's *t*-test or one-way ANOVA followed by post-hoc comparisons using Tukey corrections.

Supplementary Material

Refer to Web version on PubMed Central for supplementary material.

ACKNOWLEDGEMENTS

We thank Dr. Steven Jones from University of Louisville for providing *Ogt*-flox mice and Dr. Alison Xu from University of California at San Francisco for donating *AgRP*-Cre mice. This work was supported by NIH R01 DK089098, American Diabetes Association, and Ellison Medical Foundation to X.Y., American Heart Association to H.-B.R., NIH DP1 DK006850 and ADA Mentor-Based Fellowship to T.L.H., CNPq/Brazil to M.O.D. and M.R.Z.

REFERENCES

Andrews ZB, Liu ZW, Walllingford N, Erion DM, Borok E, Friedman JM, Tschop MH, Shanabrough M, Cline G, Shulman GI, et al. UCP2 mediates ghrelin's action on NPY/AgRP neurons by lowering free radicals. Nature. 2008; 454:846–851. [PubMed: 18668043]

Apfelbaum M, Bostsarron J, Lacatis D. Effect of caloric restriction and excessive caloric intake on energy expenditure. Am J Clin Nutr. 1971; 24:1405–1409. [PubMed: 5118011]

Arenkiel BR, Klein ME, Davison IG, Katz LC, Ehlers MD. Genetic control of neuronal activity in mice conditionally expressing TRPV1. Nature methods. 2008; 5:299–302. [PubMed: 18327266]

Bartelt A, Heeren J. Adipose tissue browning and metabolic health. Nature reviews Endocrinology. 2013

Bean BP. The action potential in mammalian central neurons. Nature reviews Neuroscience. 2007; 8:451–465. [PubMed: 17514198]

Belgardt BF, Okamura T, Bruning JC. Hormone and glucose signalling in POMC and AgRP neurons. J Physiol. 2009; 587:5305–5314. [PubMed: 19770186]

Burgi K, Cavalleri MT, Alves AS, Britto LR, Antunes VR, Michelini LC. Tyrosine hydroxylase immunoreactivity as indicator of sympathetic activity: simultaneous evaluation in different tissues of hypertensive rats. American journal of physiology Regulatory, integrative and comparative physiology. 2011; 300:R264–R271.

Chen HY, Trumbauer ME, Chen AS, Weingarth DT, Adams JR, Frazier EG, Shen Z, Marsh DJ, Feighner SD, Guan XM, et al. Orexigenic action of peripheral ghrelin is mediated by neuropeptide Y and agouti-related protein. Endocrinology. 2004; 145:2607–2612. [PubMed: 14962995]

Cheung WD, Hart GW. AMP-activated protein kinase and p38 MAPK activate O-GlcNAcylation of neuronal proteins during glucose deprivation. J Biol Chem. 2008; 283:13009–13020. [PubMed: 18353774]

Cinti S. The adipose organ at a glance. Disease models & mechanisms. 2012; 5:588–594. [PubMed: 22915020]

Cohen P, Levy JD, Zhang Y, Frontini A, Kolodin DP, Svensson KJ, Lo JC, Zeng X, Ye L, Khandekar MJ, et al. Ablation of PRDM16 and Beige Adipose Causes Metabolic Dysfunction and a Subcutaneous to Visceral Fat Switch. Cell. 2014; 156:304–316. [PubMed: 24439384]

Dentin R, Hedrick S, Xie J, Yates J 3rd, Montminy M. Hepatic glucose sensing via the CREB coactivator CRTC2. Science. 2008; 319:1402–1405. [PubMed: 18323454]

Dietrich MO, Antunes C, Geliang G, Liu ZW, Borok E, Nie Y, Xu AW, Souza DO, Gao Q, Diano S, et al. Agrp neurons mediate Sirt1's action on the melanocortin system and energy balance: roles for Sirt1 in neuronal firing and synaptic plasticity. J Neurosci. 2010; 30:11815–11825. [PubMed: 20810901]

Dietrich MO, Horvath TL. Limitations in anti-obesity drug development: the critical role of hunger-promoting neurons. Nature reviews Drug discovery. 2012; 11:675–691. [PubMed: 22858652]

Dietrich MO, Liu ZW, Horvath TL. Mitochondrial dynamics controlled by mitofusins regulate Agrp neuronal activity and diet-induced obesity. Cell. 2013; 155:188–199. [PubMed: 24074868]

Feldmann HM, Golozoubova V, Cannon B, Nedergaard J. UCP1 ablation induces obesity and abolishes diet-induced thermogenesis in mice exempt from thermal stress by living at thermoneutrality. Cell metabolism. 2009; 9:203–209. [PubMed: 19187776]

Fisher FM, Kleiner S, Douris N, Fox EC, Mepani RJ, Verdeguer F, Wu J, Kharitonenkov A, Flier JS, Maratos-Flier E, et al. FGF21 regulates PGC-1alpha and browning of white adipose tissues in adaptive thermogenesis. Genes & development. 2012; 26:271–281. [PubMed: 22302939]

Guerra C, Koza RA, Yamashita H, Walsh K, Kozak LP. Emergence of brown adipocytes in white fat in mice is under genetic control. Effects on body weight and adiposity. The Journal of clinical investigation. 1998; 102:412–420. [PubMed: 9664083]

Hahn TM, Breininger JF, Baskin DG, Schwartz MW. Coexpression of Agrp and NPY in fasting-activated hypothalamic neurons. Nature neuroscience. 1998; 1:271–272. [PubMed: 10195157]

Harms M, Seale P. Brown and beige fat: development, function and therapeutic potential. Nat Med. 2013; 19:1252–1263. [PubMed: 24100998]

Hart GW, Housley MP, Slawson C. Cycling of O-linked beta-N-acetylglucosamine on nucleocytoplasmic proteins. Nature. 2007; 446:1017–1022. [PubMed: 17460662]

Housley MP, Rodgers JT, Udeshi ND, Kelly TJ, Shabanowitz J, Hunt DF, Puigserver P, Hart GW. O-GlcNAc regulates FoxO activation in response to glucose. J Biol Chem. 2008; 283:16283–16292. [PubMed: 18420577]

Housley MP, Udeshi ND, Rodgers JT, Shabanowitz J, Puigserver P, Hunt DF, Hart GW. A PGC-1{alpha}-O-GlcNAc Transferase Complex Regulates FoxO Transcription Factor Activity in Response to Glucose. J Biol Chem. 2009; 284:5148–5157. [PubMed: 19103600]

Kajimura S, Saito M. A New Era in Brown Adipose Tissue Biology: Molecular Control of Brown Fat Development and Energy Homeostasis. Annu Rev Physiol. 2013

Kang JG, Park SY, Ji S, Jang I, Park S, Kim HS, Kim SM, Yook JI, Park YI, Roth J, et al. O-GlcNAc protein modification in cancer cells increases in response to glucose deprivation through glycogen degradation. J Biol Chem. 2009; 284:34777–34784. [PubMed: 19833729]

Kong D, Tong Q, Ye C, Koda S, Fuller PM, Krashes MJ, Vong L, Ray RS, Olson DP, Lowell BB. GABAergic RIP-Cre neurons in the arcuate nucleus selectively regulate energy expenditure. Cell. 2012; 151:645–657. [PubMed: 23101631]

Könner AC, Janoschek R, Plum L, Jordan SD, Rother E, Ma X, Xu C, Enriori P, Hampel B, Barsh GS, et al. Insulin action in AgRP-expressing neurons is required for suppression of hepatic glucose production. Cell Metab. 2007; 5:438–449. [PubMed: 17550779]

Li MD, Ruan HB, Hughes ME, Lee JS, Singh JP, Jones SP, Nitabach MN, Yang X. O-GlcNAc signaling entrains the circadian clock by inhibiting BMAL1/CLOCK ubiquitination. Cell Metab. 2013; 17:303–310. [PubMed: 23395176]

Liu T, Kong D, Shah BP, Ye C, Koda S, Saunders A, Ding JB, Yang Z, Sabatini BL, Lowell BB. Fasting activation of AgRP neurons requires NMDA receptors and involves spinogenesis and increased excitatory tone. Neuron. 2012; 73:511–522. [PubMed: 22325203]

Love DC, Hanover JA. The hexosamine signaling pathway: deciphering the "O-GlcNAc code". Sci STKE. 2005; 2005:re13. [PubMed: 16317114]

Luquet S, Perez FA, Hnasko TS, Palmiter RD. NPY/AgRP neurons are essential for feeding in adult mice but can be ablated in neonates. Science. 2005; 310:683–685. [PubMed: 16254186]

Luquet S, Phillips CT, Palmiter RD. NPY/AgRP neurons are not essential for feeding responses to glucoprivation. Peptides. 2007; 28:214–225. [PubMed: 17194499]

McClain DA, Lubas WA, Cooksey RC, Hazel M, Parker GJ, Love DC, Hanover JA. Altered glycan-dependent signaling induces insulin resistance and hyperleptinemia. Proc Natl Acad Sci U S A. 2002; 99:10695–10699. [PubMed: 12136128]

Nedergaard J, Bengtsson T, Cannon B. Three years with adult human brown adipose tissue. Ann N Y Acad Sci. 2010; 1212:E20–E36. [PubMed: 21375707]

Nedergaard J, Cannon B. UCP1 mRNA does not produce heat. Biochim Biophys Acta. 2013; 1831:943–949. [PubMed: 23353596]

Nogueiras R, Wilson H, Rohner-Jeanrenaud F, Tschop MH. Central nervous system regulation of adipocyte metabolism. Regulatory peptides. 2008; 149:26–31. [PubMed: 18453013]

Petrovic N, Walden TB, Shabalina IG, Timmons JA, Cannon B, Nedergaard J. Chronic peroxisome proliferator-activated receptor gamma (PPARgamma) activation of epididymally derived white adipocyte cultures reveals a population of thermogenically competent, UCP1-containing adipocytes molecularly distinct from classic brown adipocytes. J Biol Chem. 2010; 285:7153–7164. [PubMed: 20028987]

Qian S, Chen H, Weingarth D, Trumbauer ME, Novi DE, Guan X, Yu H, Shen Z, Feng Y, Frazier E, et al. Neither agouti-related protein nor neuropeptide Y is critically required for the regulation of energy homeostasis in mice. Mol Cell Biol. 2002; 22:5027–5035. [PubMed: 12077332]

Qian SW, Tang Y, Li X, Liu Y, Zhang YY, Huang HY, Xue RD, Yu HY, Guo L, Gao HD, et al. BMP4-mediated brown fat-like changes in white adipose tissue alter glucose and energy homeostasis. Proc Natl Acad Sci U S A. 2013; 110:E798–E807. [PubMed: 23388637]

Rosen ED, Spiegelman BM. What We Talk About When We Talk About Fat. Cell. 2014; 156:20–44. [PubMed: 24439368]

Ruan HB, Han X, Li MD, Singh JP, Qian K, Azarhoush S, Zhao L, Bennett AM, Samuel VT, Wu J, et al. O-GlcNAc transferase/host cell factor C1 complex regulates gluconeogenesis by modulating PGC-1alpha stability. Cell Metab. 2012; 16:226–237. [PubMed: 22883232]

Ruan HB, Nie Y, Yang X. Regulation of Protein Degradation by O-GlcNAcylation: Crosstalk with Ubiquitination. Mol Cell Proteomics. 2013a; 12:3489–3497. [PubMed: 23824911]

Ruan HB, Singh JP, Li MD, Wu J, Yang X. Cracking the O-GlcNAc code in metabolism. Trends Endocrinol Metab. 2013b; 24:301–309. [PubMed: 23647930]

Sanz E, Yang L, Su T, Morris DR, McKnight GS, Amieux PS. Cell-type-specific isolation of ribosome-associated mRNA from complex tissues. Proc Natl Acad Sci U S A. 2009; 106:13939–13944. [PubMed: 19666516]

Scherer T, Buettner C. Yin and Yang of hypothalamic insulin and leptin signaling in regulating white adipose tissue metabolism. Reviews in endocrine & metabolic disorders. 2011; 12:235–243. [PubMed: 21713385]

Seale P, Conroe HM, Estall J, Kajimura S, Frontini A, Ishibashi J, Cohen P, Cinti S, Spiegelman BM. Prdm16 determines the thermogenic program of subcutaneous white adipose tissue in mice. The Journal of clinical investigation. 2011; 121:96–105. [PubMed: 21123942]

Shafi R, Iyer SP, Ellies LG, O'Donnell N, Marek KW, Chui D, Hart GW, Marth JD. The O-GlcNAc transferase gene resides on the X chromosome and is essential for embryonic stem cell viability and mouse ontogeny. Proc Natl Acad Sci U S A. 2000; 97:5735–5739. [PubMed: 10801981]

Shi YC, Lau J, Lin Z, Zhang H, Zhai L, Sperk G, Heilbronn R, Mietzsch M, Weger S, Huang XF, et al. Arcuate NPY controls sympathetic output and BAT function via a relay of tyrosine hydroxylase neurons in the PVN. Cell Metab. 2013; 17:236–248. [PubMed: 23395170]

Shibata H, Bukowiecki LJ. Regulatory alterations of daily energy expenditure induced by fasting or overfeeding in unrestrained rats. Journal of applied physiology. 1987; 63:465–470. [PubMed: 3477537]

Small CJ, Kim MS, Stanley SA, Mitchell JR, Murphy K, Morgan DG, Ghatei MA, Bloom SR. Effects of chronic central nervous system administration of agouti-related protein in pair-fed animals. Diabetes. 2001; 50:248–254. [PubMed: 11272133]

Smorlesi A, Frontini A, Giordano A, Cinti S. The adipose organ: white-brown adipocyte plasticity and metabolic inflammation. Obes Rev. 2012; 2(13 Suppl):83–96. [PubMed: 23107262]

Spiegelman BM, Flier JS. Obesity and the regulation of energy balance. Cell. 2001; 104:531–543. [PubMed: 11239410]

Takahashi KA, Cone RD. Fasting induces a large, leptin-dependent increase in the intrinsic action potential frequency of orexigenic arcuate nucleus neuropeptide Y/Agouti-related protein neurons. Endocrinology. 2005; 146:1043–1047. [PubMed: 15591135]

Taylor RP, Parker GJ, Hazel MW, Soesanto Y, Fuller W, Yazzie MJ, McClain DA. Glucose deprivation stimulates O-GlcNAc modification of proteins through up-regulation of O-linked N-acetylglucosaminyltransferase. J Biol Chem. 2008; 283:6050–6057. [PubMed: 18174169]

Torres CR, Hart GW. Topography and polypeptide distribution of terminal N-acetylglucosamine residues on the surfaces of intact lymphocytes. Evidence for O-linked GlcNAc. J Biol Chem. 1984; 259:3308–3317. [PubMed: 6421821]

Trinidad JC, Barkan DT, Gulledge BF, Thalhammer A, Sali A, Schoepfer R, Burlingame AL. Global identification and characterization of both O-GlcNAcylation and phosphorylation at the murine synapse. Mol Cell Proteomics. 2012; 11:215–229. [PubMed: 22645316]

Tschop MH, Speakman JR, Arch JR, Auwerx J, Bruning JC, Chan L, Eckel RH, Farese RV Jr, Galgani JE, Hambly C, et al. A guide to analysis of mouse energy metabolism. Nature methods. 2012; 9:57–63. [PubMed: 22205519]

Vogt MC, Bruning JC. CNS insulin signaling in the control of energy homeostasis and glucose metabolism - from embryo to old age. Trends Endocrinol Metab. 2013; 24:76–84. [PubMed: 23265947]

Welle S, Campbell RG. Stimulation of thermogenesis by carbohydrate overfeeding. Evidence against sympathetic nervous system mediation. J Clin Invest. 1983; 71:916–925. [PubMed: 6339561]

Whelan SA, Dias WB, Thiruneelakantapillai L, Lane MD, Hart GW. Regulation of insulin receptor substrate 1 (IRS-1)/AKT kinase-mediated insulin signaling by O-Linked beta-N-acetylglucosamine in 3T3-L1 adipocytes. J Biol Chem. 2010; 285:5204–5211. [PubMed: 20018868]

Wiedmer P, Strasser F, Horvath TL, Blum D, Dimarchi R, Lutz T, Schurmann A, Joost HG, Tschop MH, Tong J. Ghrelin-induced hypothermia: a physiological basis but no clinical risk. Physiology & behavior. 2011; 105:43–51. [PubMed: 21513721]

Wilkinson KD, Lee KM, Deshpande S, Duerksen-Hughes P, Boss JM, Pohl J. The neuron-specific protein PGP 9.5 is a ubiquitin carboxyl-terminal hydrolase. Science. 1989; 246:670–673. [PubMed: 2530630]

Wu J, Bostrom P, Sparks LM, Ye L, Choi JH, Giang AH, Khandekar M, Virtanen KA, Nuutila P, Schaart G, et al. Beige adipocytes are a distinct type of thermogenic fat cell in mouse and human. Cell. 2012; 150:366–376. [PubMed: 22796012]

Wu J, Cohen P, Spiegelman BM. Adaptive thermogenesis in adipocytes: is beige the new brown? Genes Dev. 2013; 27:234–250. [PubMed: 23388824]

Xu AW, Kaelin CB, Takeda K, Akira S, Schwartz MW, Barsh GS. PI3K integrates the action of insulin and leptin on hypothalamic neurons. J Clin Invest. 2005; 115:951–958. [PubMed: 15761497]

Yang X, Ongusaha PP, Miles PD, Havstad JC, Zhang F, So WV, Kudlow JE, Michell RH, Olefsky JM, Field SJ, et al. Phosphoinositide signalling links O-GlcNAc transferase to insulin resistance. Nature. 2008; 451:964–969. [PubMed: 18288188]

Yang X, Zhang F, Kudlow JE. Recruitment of O-GlcNAc transferase to promoters by corepressor mSin3A: coupling protein O-GlcNAcylation to transcriptional repression. Cell. 2002; 110:69–80. [PubMed: 12150998]

Yang Y, Atasoy D, Su HH, Sternson SM. Hunger states switch a flip-flop memory circuit via a synaptic AMPK-dependent positive feedback loop. Cell. 2011; 146:992–1003. [PubMed: 21925320]

Yasuda T, Masaki T, Kakuma T, Yoshimatsu H. Hypothalamic melanocortin system regulates sympathetic nerve activity in brown adipose tissue. Experimental biology and medicine. 2004; 229:235–239. [PubMed: 14988515]

Highlights

- Fasting and activation of AgRP neurons suppress browning of selected fat depots.
- OGT in AgRP neurons is required for suppression of browning induced by fasting.
- OGT targets $K_V7.3$ potassium channel to regulate AgRP neuronal firing.
- Deletion of OGT in AgRP neurons protects mice from diet-induced obesity.

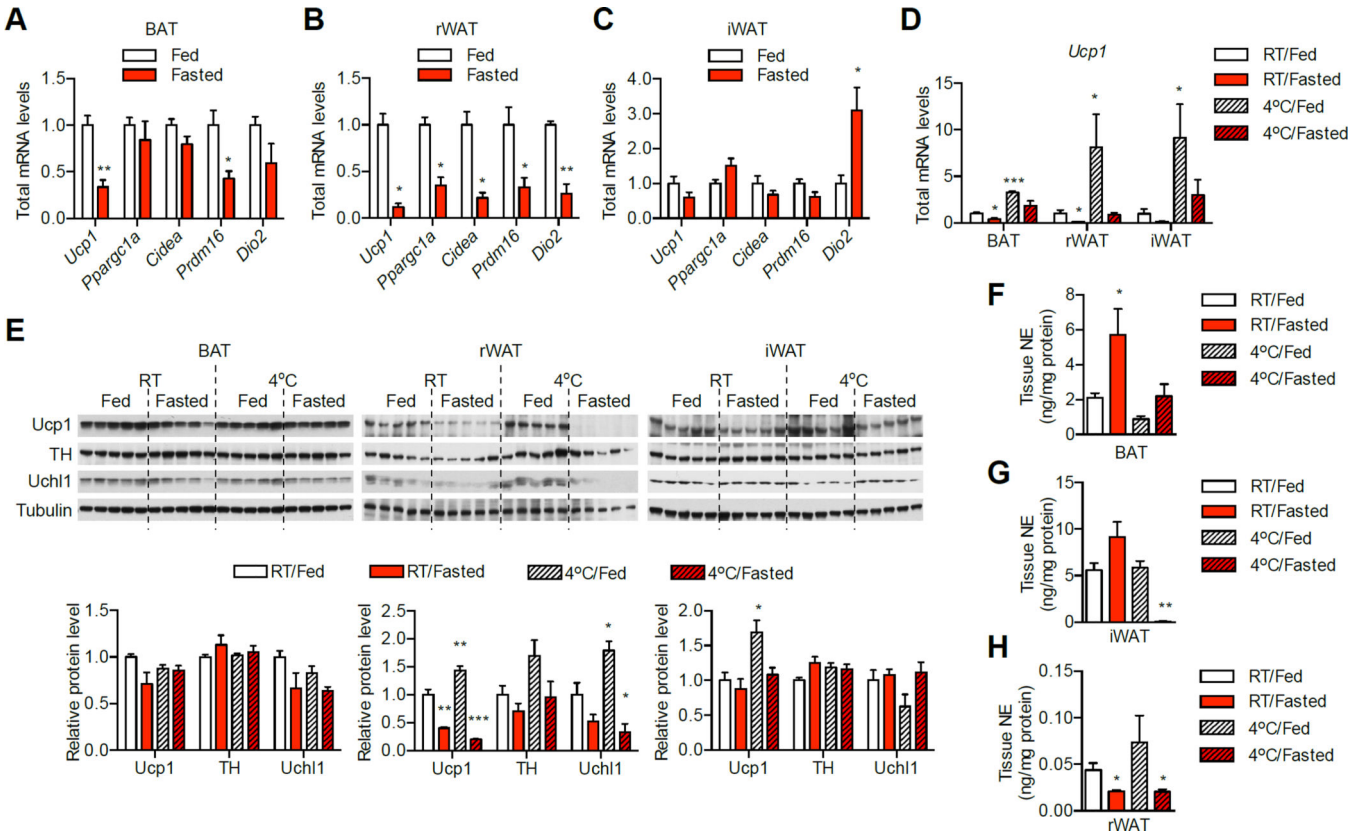

Figure 1. Fasting and AgRP neurons suppress WAT browning

(A–C) Expression of thermogenic genes in different fat depots from *ad libitum* fed or 24 h-fasted mice (n = 5). Same amount of RNA was used for reverse transcription followed by real time PCR. Gene expression was first normalized to *36b4* and then relative mRNA amount per depot was calculated based on total RNA levels (Figure S1A). Total levels of thermogenic genes per depot in BAT (A), rWAT (B) and iWAT (C) are shown.

(D–H) Mice were either fed *ad libitum* or fasted overnight at room temperature (RT) or 4 °C. (D) Expression of *Ucp1* transcript in different fat depots (n = 5). (E) Immunoblotting showing protein levels of Ucp1, TH, and Uchl1. Densitometric analyses are shown at the bottom. (F–H) NE levels in (F) BAT, (G) iWAT, and (H) rWAT. Data are shown as mean ± SEM. *, $p < 0.01$; **, $p < 0.01$ by unpaired student's *t*-test. See also Figure S1.

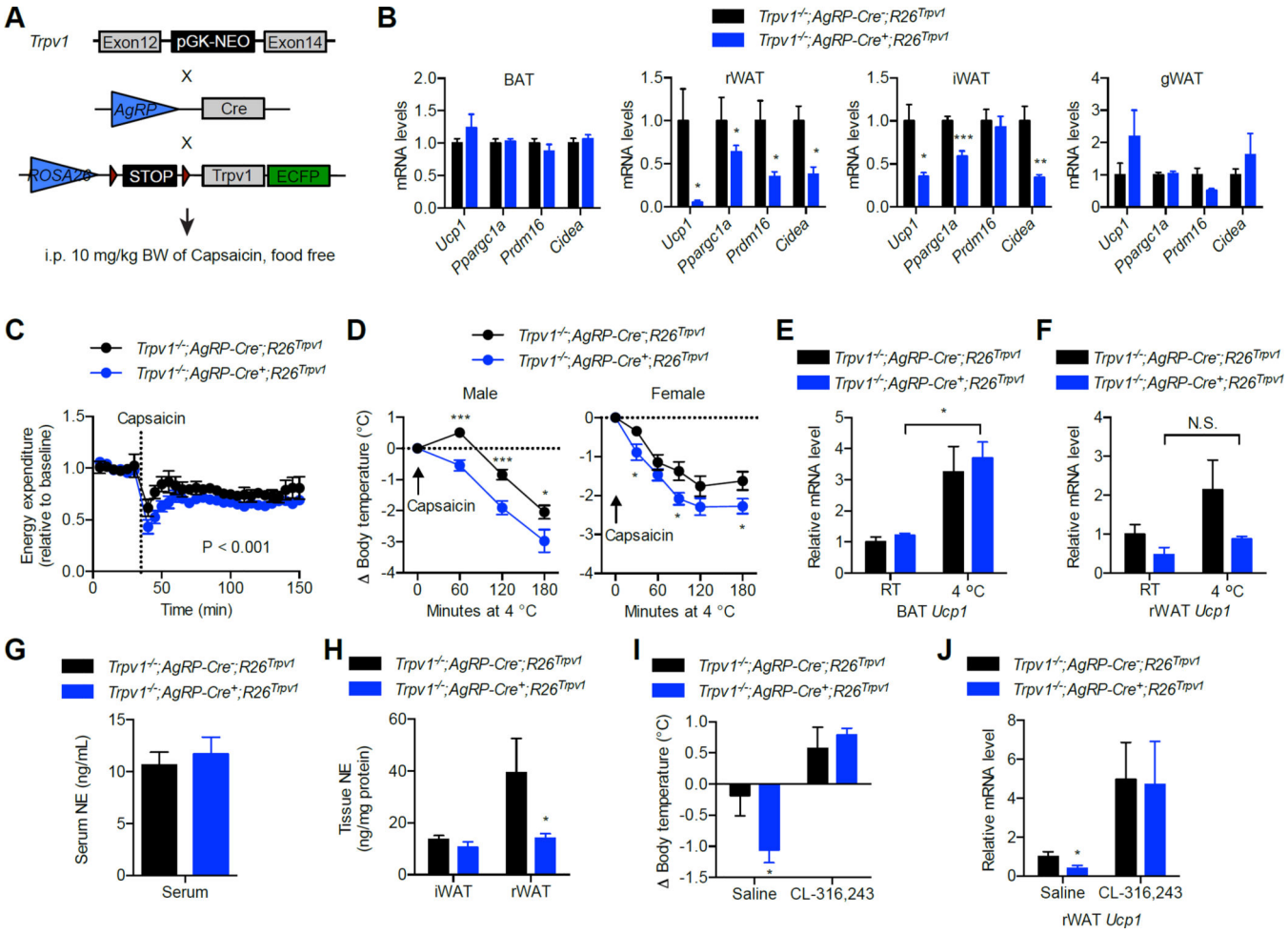

Figure 2. Acute activation of AgRP neurons suppresses the thermogenic program in WAT

(A) 10 mg/kg body weight of capsaicin was injected to *Trpv1*$^{-/-}$*;AgRP-Cre*$^{-}$*;R26*^{Trpv1} (control) or *Trpv1*$^{-/-}$*;AgRP-Cre*$^{+}$*;R26*^{Trpv1} transgenic mice. Food was removed during all the experiments.

(B) Thermogenic gene expression in adipose tissues, 1 h after capsaicin injection (n = 4).

(C) Changes in energy expenditure of mice after capsaicin injection (n = 4).

(D) Body temperature of mice during cold challenge immediately after capsaicin injection (n = 9–11).

(E, F) *Ucp1* expression in BAT (E) and rWAT (F) of capsaicin-injected mice at RT or 4 °C for 2h (n = 4–6).

(G) Serum levels of NE of mice after 2h of capsaicin injection (n = 8).

(H) Levels of NE in iWAT and rWAT of mice after 2h of capsaicin injection (n = 8).

(I, J) Mice were injected with saline or 1 mg/kg body weight of CL-316, 243 at the same time with capsaicin. (I) Change in core body temperature (n = 6–8). (J) Levels of *Ucp1* transcript in rWAT (n = 4–6). Data are shown as mean ± SEM. *, $p < 0.05$; **, $p < 0.01$; ***, $p < 0.001$ by unpaired student's *t*-tests.

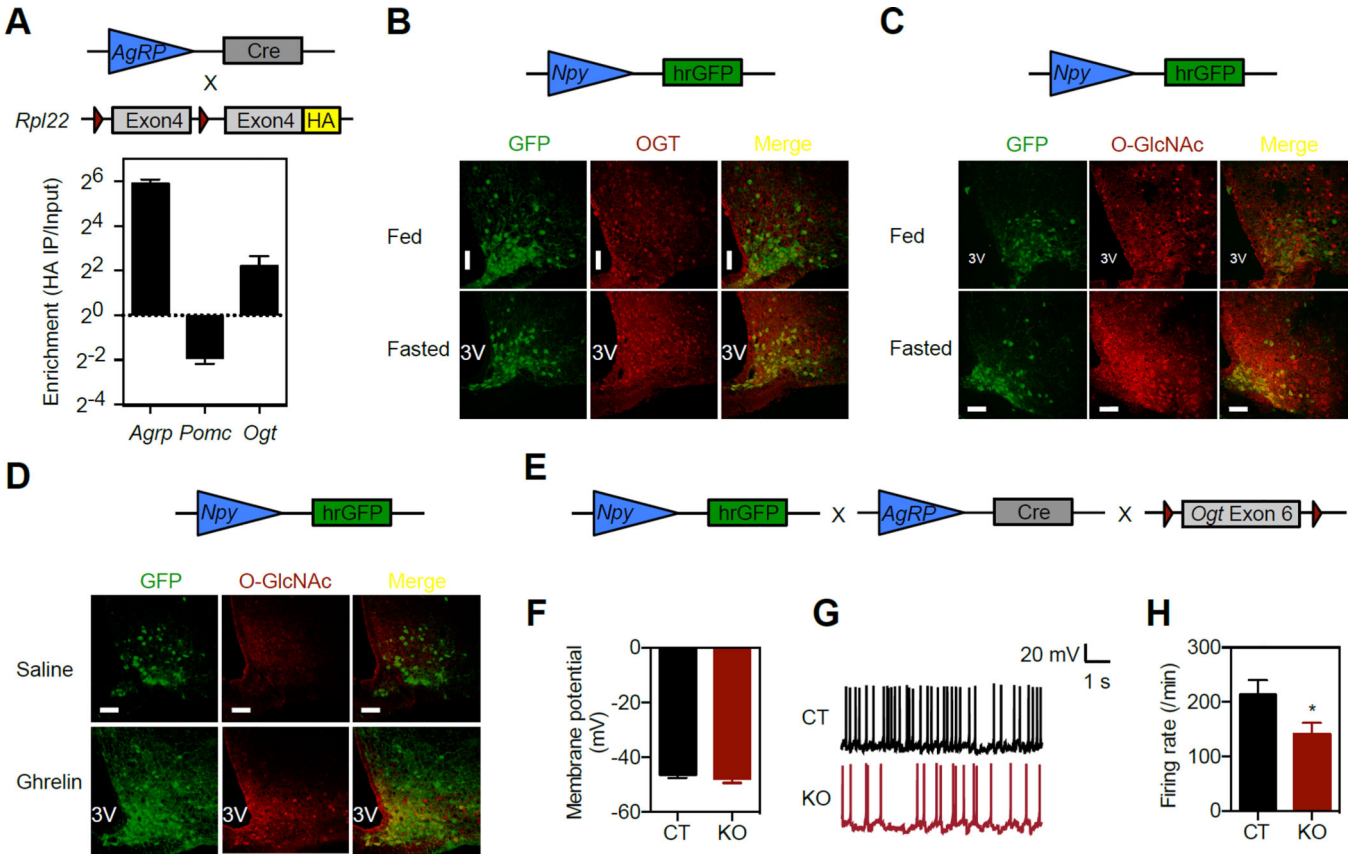

Figure 3. OGT is required for AgRP neuron activity

(A) Ribosome-associated mRNAs were isolated from the acuate nucleus of *AgRP-Cre*$^{+}$*; RPL22*^{HA} mice, and real-time PCR was performed to determine the enrichment of *Ogt* transcripts in HA immunoprecipitation compared to the input (n = 4). *Agrp* and *Pomc* transcripts were used as controls.

(B) Immunostaining of OGT in the hypothalamus of fed and overnight-fasted *Npy-hrGFP* mice.

(C) Immunostaining of O-GlcNAc in the hypothalamus of fed and overnight-fasted *Npy-hrGFP* mice.

(D) Immunostaining of O-GlcNAc in the hypothalamus of *Npy-hrGFP* mice injected with saline or 120 mmol/kg body weight of ghrelin for 1 h.

(E) *AgRP-Cre*$^{-}$*;Ogt*^{flox} (CT) and *AgRP-Cre*$^{+}$*;Ogt*^{flox} (KO) mice were crossbred onto *Npy-hrGFP* background for the whole-cell current-clamp recordings.

(F) Basal membrane potential of AgRP neurons (n = 19).

(G) Representative tracing of action potentials of AgRP neurons.

(H) Firing rate of AgRP neurons (n = 19). Data are shown as mean ± SEM. *, $p < 0.05$ by unpaired student's *t*-test. 3V, 3rd ventricle. Bar = 50 μm. See also Figure S2.

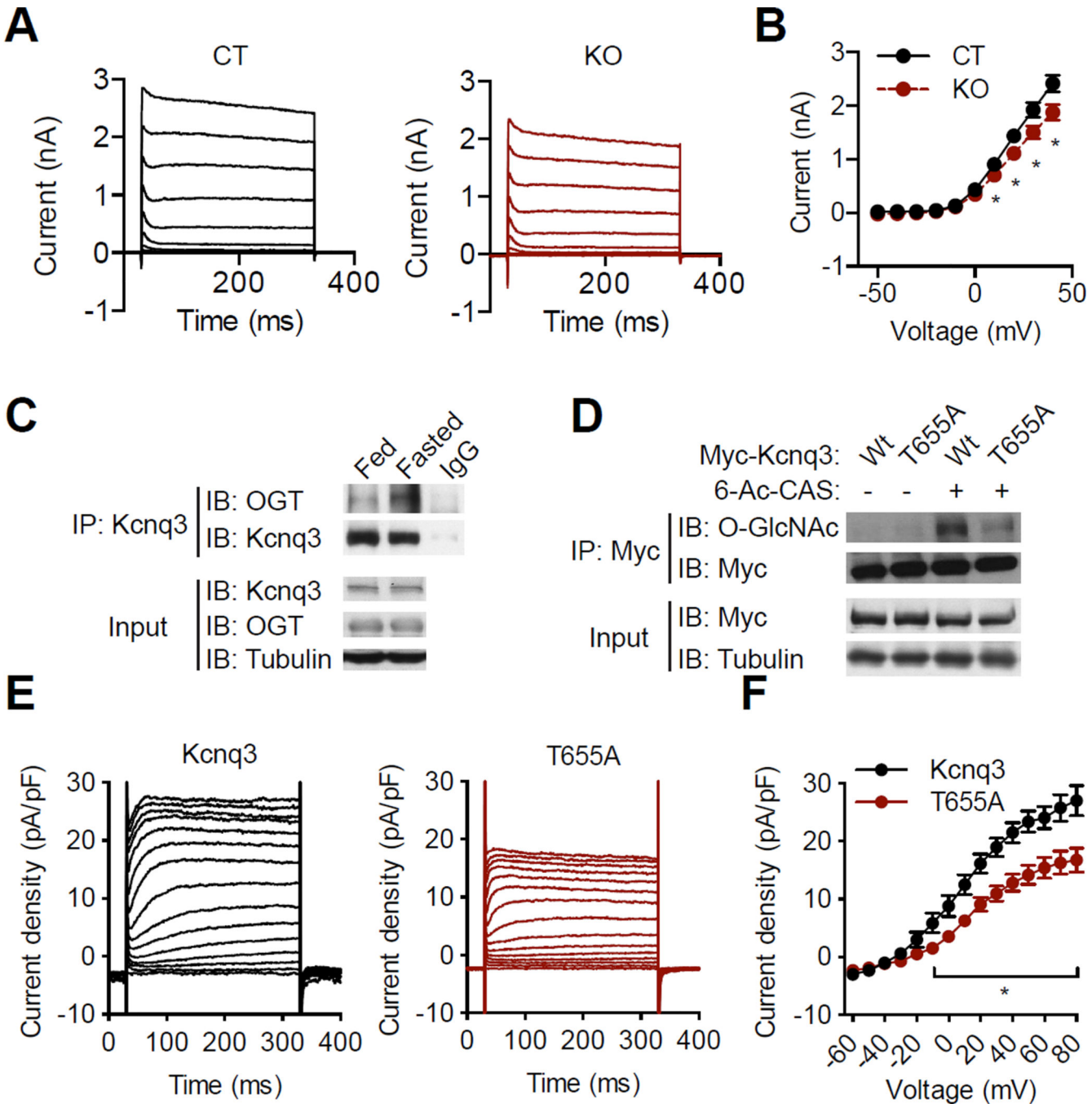

Figure 4. O-GlcNAcylation modulates the voltage-dependent Kcnq3 channel

(A) 10 mV- stepwise whole-cell voltage-clamp (-50 mV to 40 mV) was performed to record K^+ current in *Npy-hrGFP-positive* cells (n = 6–8).

(B) Current-voltage curve of K^+ currents at 300 ms in panel A.

(C) Immunoprecipitation showing interaction between OGT and Kcnq3 in fed and fasted hypothalamus.

(D) Myc-tagged wildtype and T655A Kcnq3 were expressed in HEK 293 cells. O-GlcNAc levels were determined by Myc immunoprecipitation followed by western blotting. 6-Ac-CAS, a specific inhibitor of O-GlcNAcase to increase O-GlcNAc levels.

(E) HEK 293 cells were transfected with wildtype or T655A Kcnq, K^+ currents were recorded by whole-cell voltage-clamp (-60 to 80 mV), and then current density was calculated.

(F) Current density - voltage curve of wildtype and T655A Kcnq3 at 300 ms in E. Data are shown as mean ± SEM. *, $p < 0.05$ by unpaired student's *t*-test

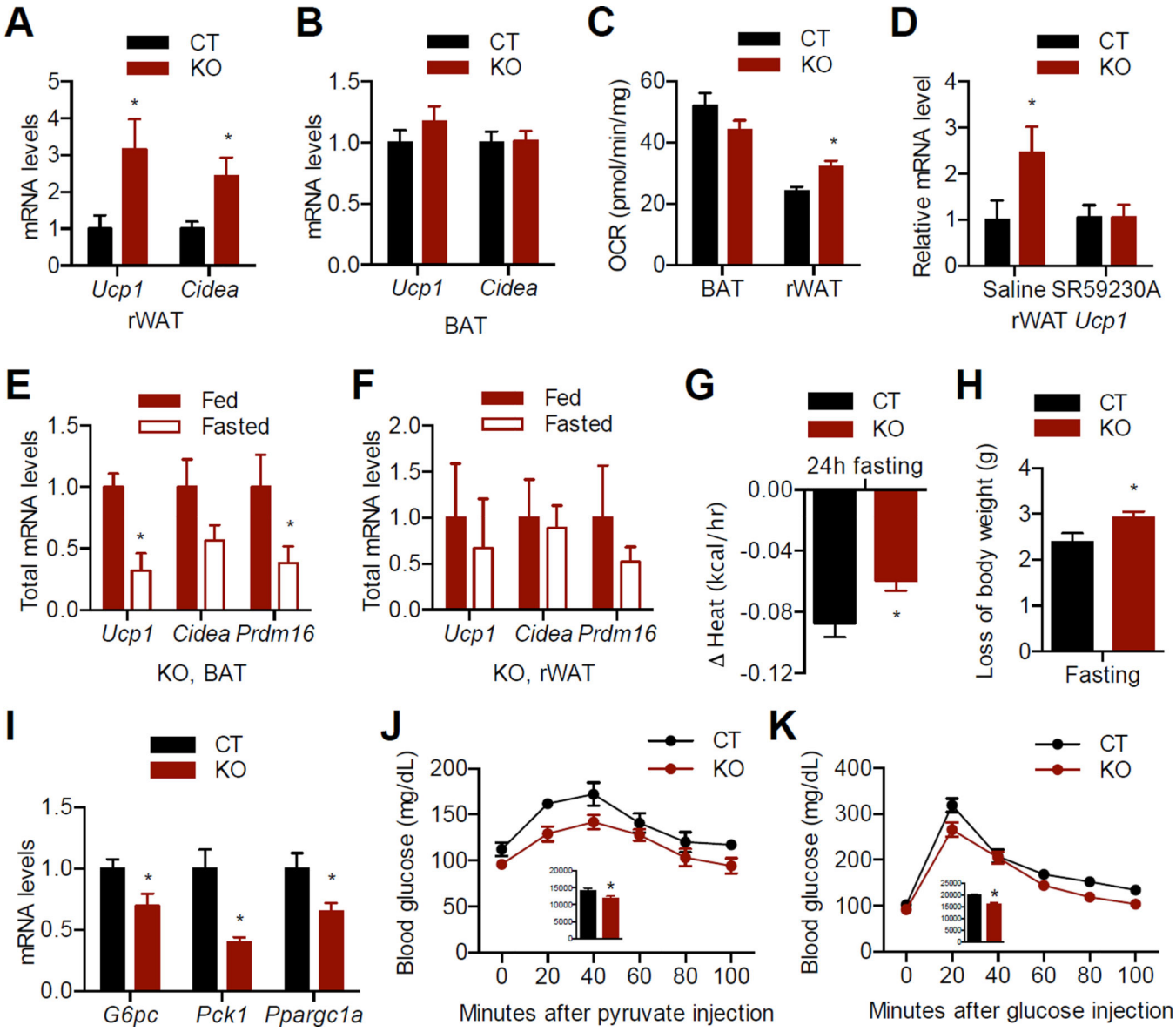

Figure 5. Loss of *Ogt* in AgRP neurons promotes browning and improves glucose metabolism in mice fed on normal chow

(A, B) Expression of thermogenic genes in rWAT (A) and BAT (B) of 6-month-old female mice (n = 4).

(C) Oxygen consumption rate of BAT and rWAT in the presence of oligomycin, an ATPase inhibitor (n = 8).

(D) Expression of *Ucp1* in rWAT from mice treated with 3 days of saline or SR59230A (n = 4–6).

(E–F) Expression of thermogenic genes in BAT (E) and rWAT (F) from fed and 24 h-fasted AgRP-OGT KO female mice (n = 3–4). Total amounts of mRNA were calculated based on relative mRNA levels and total amounts of RNA isolated. (G, H) Loss of energy expenditure (G) and body weight (H) in CT and KO female mice after fasting for 24 h (n = 6–15).

(I) Expression of gluconeogenic genes in liver of 6-month-old female mice (n = 3–4). (J) Pyruvate tolerance test in 5-month-old female mice (n = 4–7). Insert, area under curve (AUC). (K) Glucose tolerance test in 5-month-old female mice (n = 8–12). Insert, AUC. Data are shown as mean ± SEM. *, $p < 0.05$ by unpaired student's *t*-test. See also Figure S3.

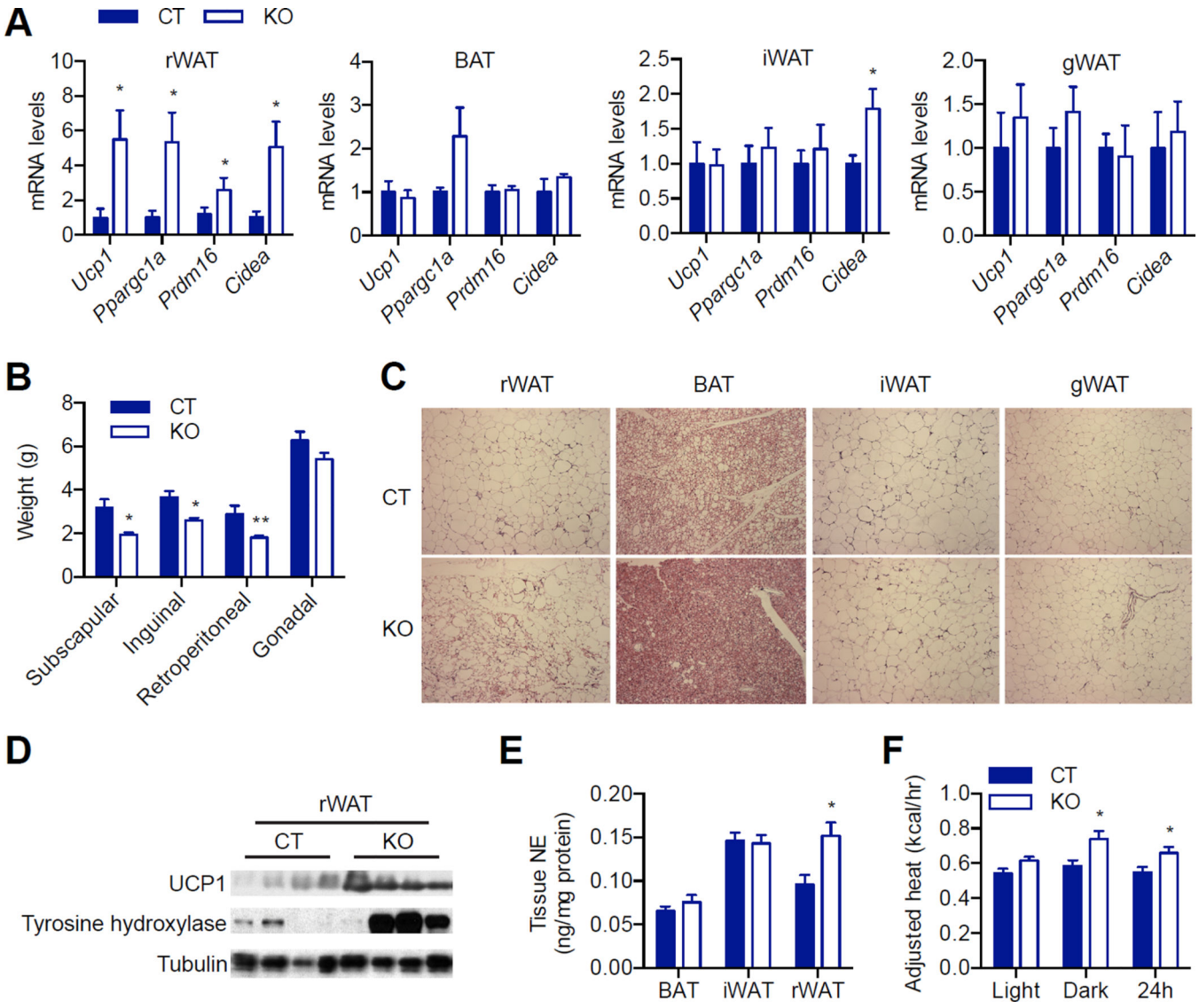

Figure 6. Browning phenotypes in *AgRP-Ogt* mice on HFD

(A) Thermogenic gene expression in different fat depots from 10-month-old female HFD mice (n = 5–7).

(B) Weight of fat depots in 10-month-old female HFD mice (n = 5–6).

(C) H&E staining of adipose tissues from 10-month-old female HFD mice.

(D) Immunoblotting of UCP1 and tyrosine hydroxylase in rWAT of 10-month-old female HFD mice.

(E) Norepinephrine levels in fat depots (n = 12).

(F) Energy expenditure in 6-month-old female HFD mice determined by metabolic cage study followed by regressing to body weight using ANCOVA analysis (n = 11). Data are shown as mean ± SEM. *, $p < 0.05$; **, $p < 0.01$ by unpaired student's *t*-test.

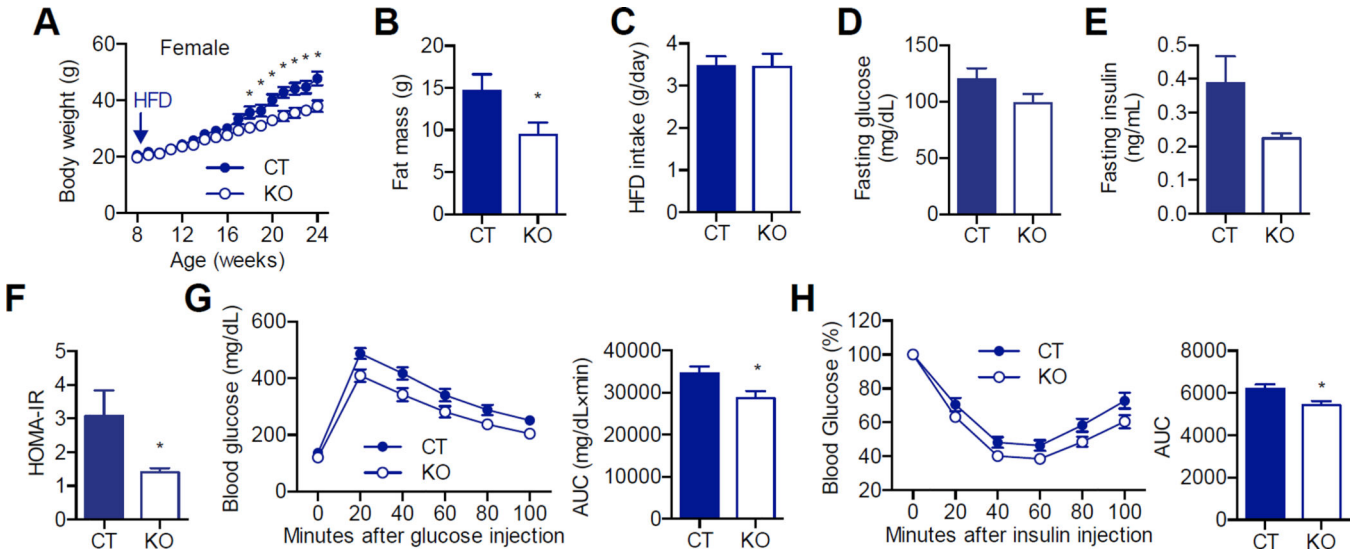

Figure 7. Loss of *Ogt* in AgRP neurons protects mice from diet-induced obesity and insulin resistance

(A) Growth curve of female mice fed with HFD (n =12–13).

(B) Fat mass of 5-month-old female HFD mice (n =12–13).

(C) Daily intake of HFD in 2-month-old female mice (n = 6).

(D–F) Fasting blood glucose (D), fasting serum insulin (E), and HOMA-IR (F) in 6-month-old female HFD mice (n = 6).

(G) Glucose tolerance test in 5-month-old female HFD mice. Area under curve (AUC) is shown to the right (n = 17–19).

(H) Insulin tolerance test in 5-month-old female HFD mice. Area under curve (AUC) is shown to the right (n = 12–13). Data are shown as mean ± SEM. *, $p < 0.05$ by unpaired student's *t*-test.

See also Figure S4.